

Updated Constraints on the Minimal Supergravity Model

Howard Baer, Csaba Balázs, Alexander Belyaev*

Department of Physics, Florida State University

Tallahassee, FL, USA 32306

E-mail: baer@hep.fsu.edu, balazs@hep.fsu.edu, belyaev@hep.fsu.edu

J. Kenichi Mizukoshi

Instituto de Física, Universidade de São Paulo

C.P. 66318, 05315-970, São Paulo, Brazil.

E-mail: mizuka@fma.if.usp.br

Xerxes Tata, Yili Wang

Department of Physics and Astronomy, University of Hawaii,

Honolulu, HI 96822, USA

E-mail: tata@phys.hawaii.edu, yili@phys.hawaii.edu

ABSTRACT: Recently, refinements have been made on both the theoretical and experimental determinations of *i.)* the mass of the lightest Higgs scalar (m_h), *ii.)* the relic density of cold dark matter in the universe ($\Omega_{CDM}h^2$), *iii.)* the branching fraction for radiative B decay $BF(b \rightarrow s\gamma)$, *iv.)* the muon anomalous magnetic moment (a_μ), and *v.)* the flavor violating decay $B_s \rightarrow \mu^+\mu^-$. Each of these quantities can be predicted in the MSSM, and each depends in a non-trivial way on the spectra of SUSY particles. In this paper, we present updated constraints from each of these quantities on the minimal supergravity (mSUGRA) model as embedded in the computer program ISAJET. The combination of constraints points to certain favored regions of model parameter space where collider and non-accelerator SUSY searches may be more focussed.

KEYWORDS: Supersymmetry Phenomenology, Supersymmetric Standard Model, Dark Matter, Rare Decays.

*On leave of absence from Nuclear Physics Institute, Moscow State University.

1. Introduction

The search for weak scale supersymmetric matter is one of the prime objectives of present and future collider experiments. Particle physics models including supersymmetry solve a host of problems occurring in non-supersymmetric theories, and predict a variety of new matter states—the sparticles—at or around the TeV scale[1]. Supersymmetric models can be classified by the mechanism for communicating SUSY breaking from the hidden sector to the observable sector. Possibilities include gravity mediated SUSY breaking (SUGRA)[2], gauge mediated SUSY breaking (GMSB)[3], anomaly mediated SUSY breaking (AMSB)[4] and gaugino mediated SUSY breaking (inoMSB)[5]. Of these, the SUGRA models may be perceived as the most conservative, since they do not require the introduction of either extra dimensions or new messenger fields, and because gravity exists.

The so-called *minimal* supergravity (mSUGRA) model (sometimes also referred to as the CMSSM model) has traditionally been the most popular choice for phenomenological SUSY analyses. In mSUGRA, it is assumed that the Minimal Supersymmetric Standard Model (MSSM) is valid from the weak scale all the way up to the GUT scale $M_{GUT} \simeq 2 \times 10^{16}$ GeV, where the gauge couplings g_1 and g_2 unify. In many of the early SUGRA models[2], a simple choice of Kähler metric G_i^j and gauge kinetic function f_{AB} led to *universal* soft SUSY breaking scalar masses (m_0), gaugino masses ($m_{1/2}$) and A -terms (A_0) at M_{GUT} . This assumption of universality in the scalar sector leads to the phenomenologically required suppression of flavor violating processes that are supersymmetric in origin. However, there is no known physical principle which gives rise to the desired form of G_i^j and f_{AB} ; indeed, for general forms of G_i^j and f_{AB} , non-universal masses are expected[6]. In addition, even if nature did select a SUGRA model leading to tree level universality, quantum corrections would (without further assumptions) lead to large deviations from universality[7]. Hence, the universality assumption nowadays is regarded as being ad hoc—entirely motivated by the phenomenological need for suppression of flavor violating processes in the MSSM.

In the mSUGRA model, we thus assume universal scalar masses, gaugino masses and A -terms. We will also require that electroweak symmetry is broken radiatively (REWSB), allowing us to fix the magnitude, but not the sign, of the superpotential Higgs mass term μ so as to obtain the correct value of M_Z . Finally, we trade the bilinear soft supersymmetry breaking (SSB) parameter B for $\tan \beta$ (the ratio of Higgs field vacuum expectation values). Thus, the parameter set

$$m_0, m_{1/2}, A_0, \tan \beta, \text{ and } \text{sign}(\mu) \quad (1.1)$$

completely determines the spectrum of supersymmetric matter and Higgs fields.

In our calculations, we use the program ISASUGRA to calculate the SUSY particle mass spectrum. ISASUGRA is part of the ISAJET[8] package. Working in the \overline{DR} regularization scheme, the weak scale values of gauge and third generation Yukawa couplings are evolved via 2-loop RGEs to M_{GUT} . At M_{GUT} , universal SSB boundary conditions are imposed, and all SSB masses along with gauge and Yukawa couplings are evolved to the weak scale M_{weak} . Using an optimized scale choice $Q_{SUSY} = \sqrt{m_{\tilde{t}_L} m_{\tilde{t}_R}}$, the RG-

improved one-loop effective potential is minimized and the entire spectrum of SUSY and Higgs particles is calculated. Our values of m_h are in close accord with those generated by the FeynHiggsFast program[9]. Yukawa couplings are updated[10] to account for SUSY threshold corrections, and the entire parameter set is iteratively run between M_{weak} and M_{GUT} until a stable solution (within tolerances) is obtained.

Once the SUSY and Higgs masses and mixings are known, then a host of observables may be calculated, and compared against experimental measurements. The most important of these include:

- lower limits on sparticle and Higgs boson masses from new particle searches at LEP2,
- the relic density of neutralinos originating from the Big Bang,
- the branching fraction of the flavor changing decay $b \rightarrow s\gamma$,
- the value of muon anomalous magnetic moment $a_\mu = \frac{(g-2)_\mu}{2}$ and
- the lower bound on the rate for the rare decay $B_s \rightarrow \mu^+\mu^-$.

Our goal is to delineate the mSUGRA parameter space region consistent with all these constraints. Similar studies have recently been presented in Refs. [11, 12, 13, 14, 15]. In this report we examine these constraints using the updated ISASUGRA package, which is convenient for explicit event generation for various colliders using the ISAJET v7.63 program, which includes several improvements over previous versions. The most important of these improvements are the evaluation of the bottom Yukawa coupling and the value of m_A , especially for large values of $\tan\beta$. Complete 1-loop self energy corrections as given in Ref. [10] have been incorporated.¹ Comparisons of ISAJET v7.63 with other similar codes are available in Ref. [16].

Returning to our analysis, we also incorporate a new calculation of the neutralino relic density $\Omega_{\tilde{Z}_1} h^2$ that has recently become available[17]. In Ref. [17], all relevant neutralino annihilation and co-annihilation processes are calculated, and the neutralino relic density is evaluated using *relativistic* thermal averaging (see also Refs. [18] and recently Belanger *et al.*, Ref. [19]). The latter is especially important in evaluating the relic density when s -channel annihilation resonances occur, as in the mSUGRA model at large $\tan\beta$, when $\tilde{Z}_1\tilde{Z}_1 \rightarrow A$, $H \rightarrow f\bar{f}$, where the f s are SM fermions[18, 20, 21, 22, 23]. We also present improved $b \rightarrow s\gamma$ branching fraction predictions in accord with the current ISAJET release. We also discuss constraints imposed by the measurement of the muon anomalous magnetic moment, using updated calculations from two somewhat different analyses. Finally, we delineate the region of mSUGRA parameter space excluded by the CDF lower limit[24] on the branching fraction of $B_s \rightarrow \mu^+\mu^-$. This constraint is important only for very large values of $\tan\beta$ [25].

Within the mSUGRA framework, the parameters m_0 and $m_{1/2}$ are the most important for fixing the scale of sparticle masses. The $m_0 - m_{1/2}$ plane (for fixed values of other

¹On the technical side, the numerical precision in ISAJET has been improved to facilitate a better analysis near the boundary of the region excluded by electroweak symmetry breaking constraints.

parameters) is convenient for a simultaneous display of these constraints, and hence, of parameter regions in accord with all experimental data. Physicists interested in the mSUGRA model may wish to focus their attention on these regions. We also present five mSUGRA model cases illustrating distinctive characteristics of the mSUGRA particle spectrum for parameter choices which are consistent with all experimental constraints.

The remainder of this paper is organized as follows. In Sec. 2, we discuss the various constraints on the mSUGRA model, and present some details of our calculations. In Sec. 3, we show our main results as regions of the m_0 *vs.* $m_{1/2}$ parameter space plane for different values of $\tan\beta$ and sign of μ . Our conclusions and sample points are presented in Sec. 4.

2. Constraints and calculations in the mSUGRA model

2.1 Constraints from LEP2 searches

The LEP2 collaborations have finished taking data, and significant numbers of events were recorded at e^+e^- CM energies ranging up to $\sqrt{s} \simeq 208$ GeV. Based on negative searches for superpartners at LEP2, we require

- $m_{\tilde{W}_1} > 103.5$ GeV[26] and
- $m_{\tilde{e}_{L,R}} > 99$ GeV provided $m_{\tilde{e}} - m_{\tilde{Z}_1} < 10$ GeV[27], which is the most stringent of the slepton mass limits.

The LEP2 experiments also searched for the SM Higgs boson. In addition to finding several compelling signal candidates consistent with $m_h \sim 115$ GeV, they set a limit $m_{H_{SM}} > 114.1$ GeV[28]. In our mSUGRA parameter space scans, the lightest SUSY Higgs boson h is almost always SM-like. The exception occurs when the value of m_A becomes low, less than 100 – 150 GeV. Then there exists a near mass degeneracy between h and H , and the SM Higgs is a mixture of these. This case arises at very large values of $\tan\beta$. For clarity, we show contours where

- $m_h > 114.1$ GeV,

and will direct the reader's attention to any regions where this bound might fail.

2.2 Neutralino relic density

Measurements of galactic rotation curves, binding of galactic clusters, and the large scale structure of the universe all point to the need for significant amounts of cold dark matter (CDM) in the universe. In addition, recent measurements of the power structure of the cosmic microwave background, and measurements of distant supernovae, point to a cold dark matter density[29]

- $0.1 < \Omega_{CDM} h^2 < 0.3$.

The lightest neutralino of mSUGRA is an excellent candidate for relic CDM particles in the universe. The upper limit above represents a true constraint, while the corresponding

lower limit is flexible, since there may be additional sources of CDM such as axions, or states associated with the hidden sector and/or extra dimensions.

To estimate the relic density of neutralinos in the mSUGRA model, we use the recent calculation in Ref. [17]. In Ref. [17], all relevant neutralino annihilation and co-annihilation reactions are evaluated at tree level using the CompHEP[30] program for automatic evaluation of the associated 7618 Feynman diagrams. The annihilation cross section times velocity is relativistically thermally averaged[31], which is important for obtaining the correct neutralino relic density in the vicinity of annihilations through s -channel resonances.

2.3 The $b \rightarrow s\gamma$ branching fraction

The branching fraction $BF(b \rightarrow s\gamma)$ has recently been measured by the BELLE[32], CLEO[33] and ALEPH[34] collaborations. Combining statistical and systematic errors in quadrature, these measurements give $(3.36 \pm 0.67) \times 10^{-4}$ (BELLE), $(3.21 \pm 0.51) \times 10^{-4}$ (CLEO) and $(3.11 \pm 1.07) \times 10^{-4}$ (ALEPH). A weighted averaging of these results yields $BF(b \rightarrow s\gamma) = (3.25 \pm 0.37) \times 10^{-4}$. The 95% CL range corresponds to $\pm 2\sigma$ away from the mean. To this we should add uncertainty in the theoretical evaluation, which within the SM dominantly comes from the scale uncertainty, and is about 10%.² Together, these imply the bounds,

- $2.16 \times 10^{-4} < BF(b \rightarrow s\gamma) < 4.34 \times 10^{-4}$.

Other computations of the range of $BF(b \rightarrow s\gamma)$ include for instance Ellis *et al.*[12]: $2.33 \times 10^{-4} < BF(b \rightarrow s\gamma) < 4.15 \times 10^{-4}$, and Djouadi *et al.*[14]: $2.0 \times 10^{-4} < BF(b \rightarrow s\gamma) < 5.0 \times 10^{-4}$. In our study, we simply show contours of $BF(b \rightarrow s\gamma)$ of 2, 3, 4 and 5×10^{-4} , allowing the reader the flexibility of their own interpretation.

The calculation of $BF(b \rightarrow s\gamma)$ used here is based upon the program of Ref. [36]. That calculation uses an effective field theory approach to evaluating radiative corrections to the $b \rightarrow s\gamma$ decay rate. In running from M_{GUT} to M_{weak} , when any sparticle threshold is crossed, the corresponding sparticle is integrated out of the theory, and a new basis of decay-mediating operators multiplied by Wilson coefficients (WCs) is induced. The evolution of the WCs can be calculated by RG methods. We adopt the Anlauf procedure[37] in our calculation, which implements a tower of effective field theories, corresponding to each sparticle threshold which is crossed. This procedure sums large logarithms that can occur from a disparity between different scales involved in the loop calculations. In our calculations, we implement the running b -quark mass including SUSY threshold corrections as calculated in ISASUGRA; these effects can be important at large values of the parameter $\tan\beta$ [38, 39]. Once the relevant operators and Wilson coefficients are known at $Q = M_W$, then the SM WCs are evolved down to $Q = m_b$ via NLO RG running. At m_b , the $BF(b \rightarrow s\gamma)$ is evaluated at NLO, including bremsstrahlung effects. Our value of the SM $b \rightarrow s\gamma$ branching fraction yields 3.4×10^{-4} , with a scale uncertainty of 10%.

²We caution the reader that the SUSY contribution may have a larger theoretical uncertainty, particularly if $\tan\beta$ is large. An additional theoretical uncertainty that may increase the branching ratio in the SM is pointed out in Ref. [35].

2.4 Muon anomalous magnetic moment

The muon anomalous magnetic moment $a_\mu = \frac{(g-2)_\mu}{2}$ has been recently measured to high precision by the E821 experiment[40]: $a_\mu = 11659202(14)(6) \times 10^{-10}$. In addition, additional data analyses should soon be finished, and we may anticipate a further reduction in the experimental error by a factor of 2. The initially reported[40] 2.6σ deviation from the SM value of Ref.[41] has since been tempered somewhat by correcting the sign of the SM light-by-light contribution to a_μ [42]. A correction of the sign of the hadronic light by light contribution reduces the significance of the deviation from the SM to 1.6σ , *i.e.* at 2σ :

- $-6 < \delta a_\mu \times 10^{10} < 58$ (CM).

An alternative evaluation of theory uncertainties in the SM a_μ calculation by Melnikov[43] leads to (including the LBL correction):

- $-29.9 < \delta a_\mu \times 10^{10} < 62.3$ (Melnikov).³

In view of the theoretical uncertainty, and the impending new experimental analysis, we only present contours of δa_μ , as calculated using the program developed in [45], and leave it to the reader to decide the extent of the parameter region allowed by the data.

2.5 $B_s \rightarrow \mu^+ \mu^-$ decay

While all SUSY models contain two doublets of Higgs superfields, there are no tree level flavor changing neutral currents because one doublet \hat{H}_u couples only to $T_3 = 1/2$ fermions, while the other doublet \hat{H}_d couples just to $T_3 = -1/2$ fermions. At one loop, however, couplings of \hat{H}_u to down type fermions are induced. These induced couplings grow with $\tan\beta$. As a result, down quark Yukawa interactions and down type quark mass matrices are no longer diagonalized by the same transformation, and flavor violating couplings of neutral Higgs scalars h , H and A emerge. Of course, in the limit of large m_A , the Higgs sector becomes equivalent to the SM Higgs sector with the light Higgs boson $h = H_{SM}$, and the flavor violation decouples. The interesting thing is that while this decoupling occurs as $m_A \rightarrow \infty$, *there is no decoupling for sparticle masses becoming large*.

An important consequence of this coupling is the possibility of the decay $B_s \rightarrow \mu^+ \mu^-$, whose branching fraction has been experimentally bounded by CDF[24] to be:

- $BF(B_s \rightarrow \mu^+ \mu^-) < 2.6 \times 10^{-6}$,

mediated by the neutral states in the Higgs sector of supersymmetric models. While this branching fraction is very small within the SM ($BF_{SM}(B_s \rightarrow \mu^+ \mu^-) \simeq 3.4 \times 10^{-9}$), the amplitude for the Higgs-mediated decay of B_s grows as $\tan^3 \beta$ within the SUSY framework, and hence can completely dominate the SM contribution if $\tan \beta$ is large. Several groups[25] have analyzed the implications of this decay within the mSUGRA framework. A subset of

³Melnikov—who uses the analysis of Ref.[44] which does not use tau decay data for the evaluation of the hadronic vacuum polarization and has a more conservative error on the light by light contribution—finds $\delta a_\mu \times 10^{10} = 16.2 \pm 14.0|_{stat} \pm 6.0|_{sys} \pm 15.6|_{theory}$. The conservative “ 2σ ” range reported here can be obtained by linearly combining the theory error with the 2σ experimental error.

us[46] have recently performed an independent analysis of this decay. In the following, we use the results of this analysis to delineate the region of mSUGRA parameters excluded by the CDF upper limit on its branching fraction.

Tevatron experiments should be able to probe this decay in the near future. With an integrated sample of 2 fb^{-1} they should be sensitive to a branching fraction for $B_s \rightarrow \mu^+ \mu^-$ down to $\sim 10^{-7}$. With a still bigger data sample (that is expected to accumulate before the Large Hadron Collider begins operation) the sensitivity should be even greater.

3. Results

Our first results are plotted in Fig. 1. Here, we show the m_0 vs. $m_{1/2}$ plane for $A_0 = 0$, $\tan \beta = 10$ and $\mu < 0$. The red shaded regions are excluded either due to a lack of REWSB (right-hand side), or a stau LSP (left-hand side). The magenta region is excluded by searches for charginos and sleptons at LEP2. The region below the red contour is excluded by LEP2 Higgs searches, since here $m_h < 114.1 \text{ GeV}$. In addition, we show regions of neutralino relic density with $0.1 < \Omega_{\tilde{Z}_1} h^2 < 0.3$ (green), which is favored by cosmological observations, and also $0.3 < \Omega_{\tilde{Z}_1} h^2 < 1$ (blue) and $0.02 < \Omega_{\tilde{Z}_1} h^2 < 0.1$ (yellow). The bulk of the unshaded region in the center of the plot has $\Omega_{\tilde{Z}_1} h^2 > 1$, and would thus be excluded since the age of the universe would be less than 10 billion years. The magenta contours denote values of $BF(b \rightarrow s\gamma) = 4$ and 5×10^{-4} . Finally, the blue contours denote values of $\delta a_\mu = -30, -10, -5$ and -2×10^{-10} , moving from lower left to upper right. There is no constraint arising from $B_s \rightarrow \mu^+ \mu^-$ decay at $\tan \beta = 10$.

An intriguing feature of the plot is that the lower left green shaded region of desirable relic density, where neutralinos mainly annihilate via t -channel slepton exchange to lepton-anti-lepton pairs is essentially excluded by the m_h , $b \rightarrow s\gamma$ and δa_μ constraints. That leaves two allowed regions with a preferred relic density: one runs near the stau LSP region, where $\tilde{\tau}_1 - \tilde{Z}_1$ co-annihilation effects reduce an otherwise large relic density (as pointed out by Ellis *et al.*[47]). This region has a highly fine-tuned relic density, since a slight change in m_0 leads to either too light or too heavy of a $\tilde{\tau}_1$ mass to give $0.1 < \Omega h^2 < 0.3$ [48, 17]. The other region runs parallel to the REWSB excluded region, and occurs when the \tilde{Z}_1 has a sufficiently large higgsino component that annihilation into WW , ZZ and Zh pairs reduces the relic density[49, 17]. This region corresponds to what is known as “focus point” SUSY, and since m_0 is large, SUSY scalar masses are also large, leading to some degree of suppression of FCNC and CP violating processes[50]. The narrowness of the region indicates again that some fine-tuning of parameters is needed to achieve the right relic density, although the amount of fine-tuning is less than in the $\tilde{\tau}_1$ co-annihilation case.

A similar plot is shown in Fig. 2, but in this case for $\mu > 0$. Much of the labeling is similar to Fig. 1, although now the $b \rightarrow s\gamma$ contour denotes a branching fraction of 3×10^{-4} . In this case almost the entire plane shown is in accord with the measured branching fraction for this decay. In addition, the blue contours denote values of $\delta a_\mu = 60, 40, 20, 10, 5$ and 2×10^{-10} . Constraints from δa_μ as well as from $B_s \rightarrow \mu^+ \mu^-$ are not relevant for this case.

For $\tan \beta = 10$ and $\mu > 0$, the slepton annihilation region of relic density has a small surviving region just beyond the Higgs mass contour. For the most part, to attain a

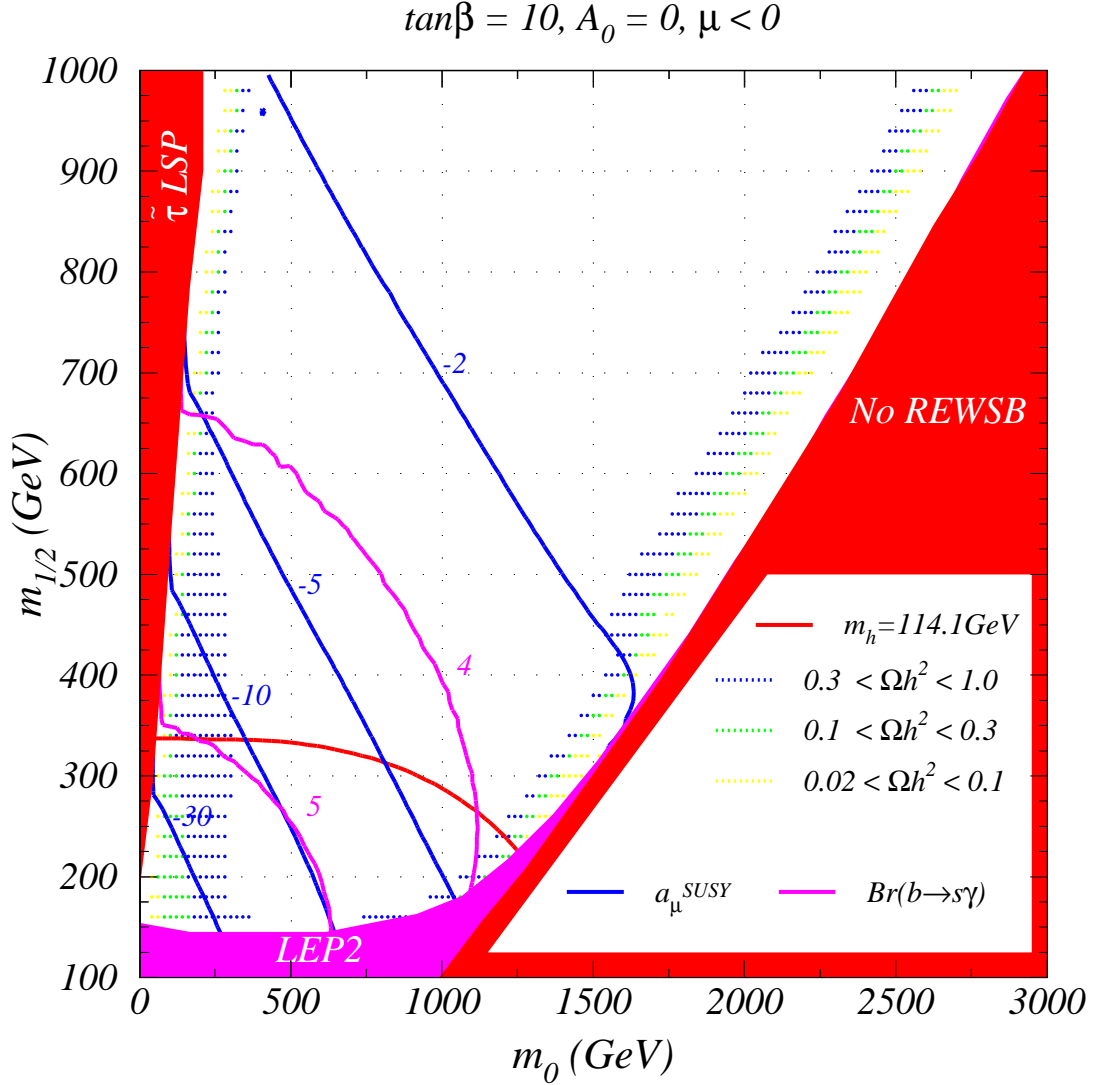


Figure 1: Plot of constraints for the mSUGRA model in the m_0 vs. $m_{1/2}$ plane for $\tan\beta = 10$, $A_0 = 0$ and $\mu < 0$. We show regions of CDM relic density, plus contours of $m_h = 114.1$ GeV, contours of muon anomalous magnetic moment a_μ ($\times 10^{10}$) and contours of $b \rightarrow s\gamma$ branching fraction ($\times 10^4$).

preferred value of neutralino relic density, one must again live in the stau co-annihilation region, or the focus point region. A final possibility is to be in the slepton annihilation region, but then the value of m_h should be slightly beyond the LEP2 limit; in this case, a Higgs boson signal may be detected in Run 2 of the Fermilab Tevatron[51].

We next turn to the m_0 vs. $m_{1/2}$ plane for $\tan\beta = 30$ and $\mu < 0$. The gray region in the bottom left corner of the plot is excluded because $m_{\tilde{\tau}_1}^2 < 0$. In this case, the area of the green region of relic density in the lower-left has expanded considerably owing to

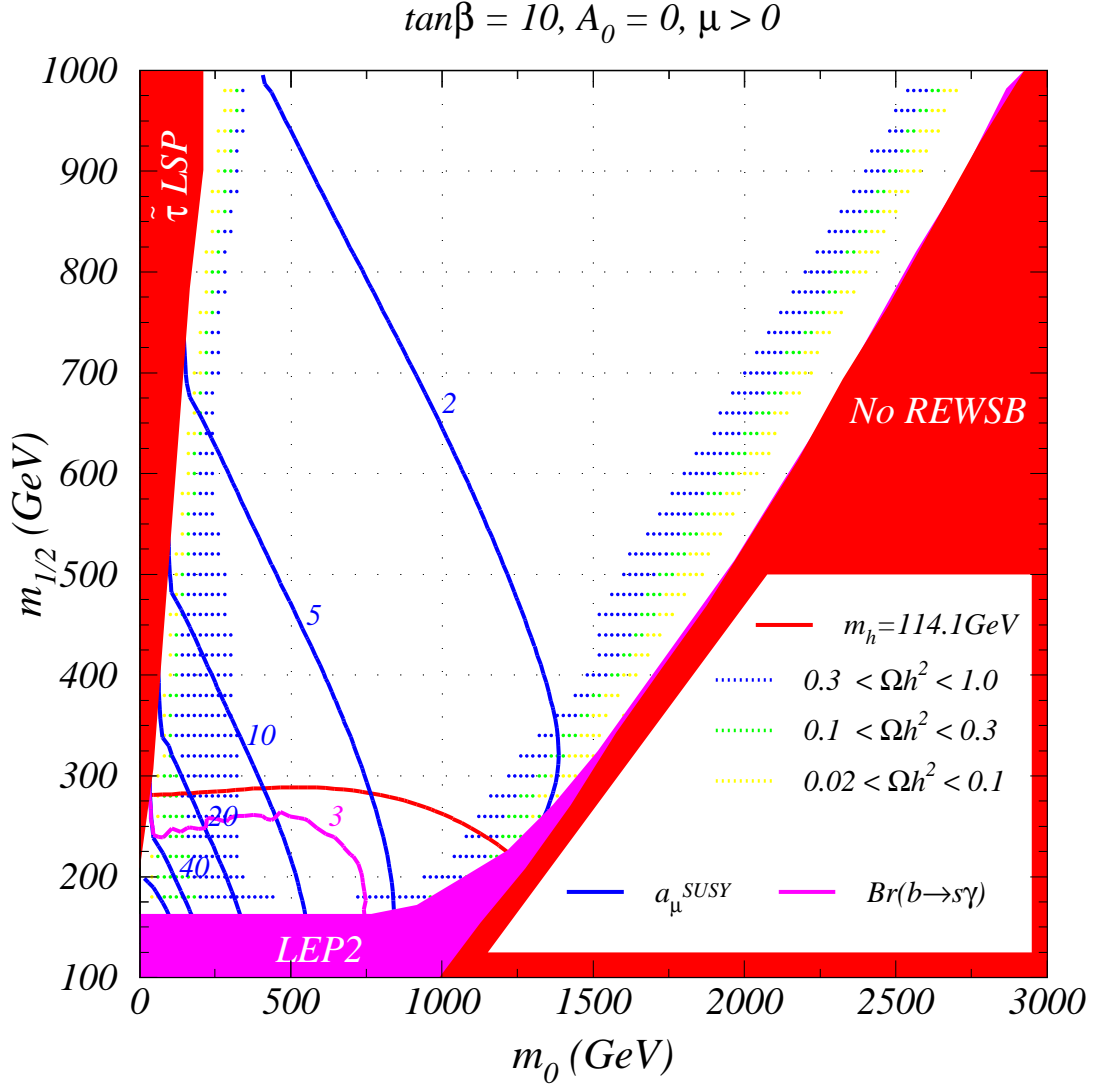


Figure 2: Same as Fig. 1, but for $\mu > 0$.

enhanced neutralino annihilation to $b\bar{b}$ and $\tau\bar{\tau}$ at large $\tan\beta$. Both lighter values of $m_{\tilde{\tau}_1}$ and $m_{\tilde{b}_1}$ and also large τ and b Yukawa couplings at large $\tan\beta$ enhance these t -channel annihilation rates through virtual staus and sbottoms. Unfortunately, the region excluded by $BF(b \rightarrow s\gamma)$ and by δa_μ (even with the conservative constraint of Ref.[43]) also expands, and most of the cosmologically preferred region is again ruled out. As before, we are left with the corridors of stau co-annihilation and the focus point scenario as the only surviving regions.

The corresponding plot is shown for $\tan\beta = 30$ but $\mu > 0$ in Figure 4. In this case, the magenta contours of $BF(b \rightarrow s\gamma)$ correspond to 2 and 3×10^{-4} . Thus, the lower left region is excluded since it leads to too low a value of $BF(b \rightarrow s\gamma)$. The δa_μ contours begin

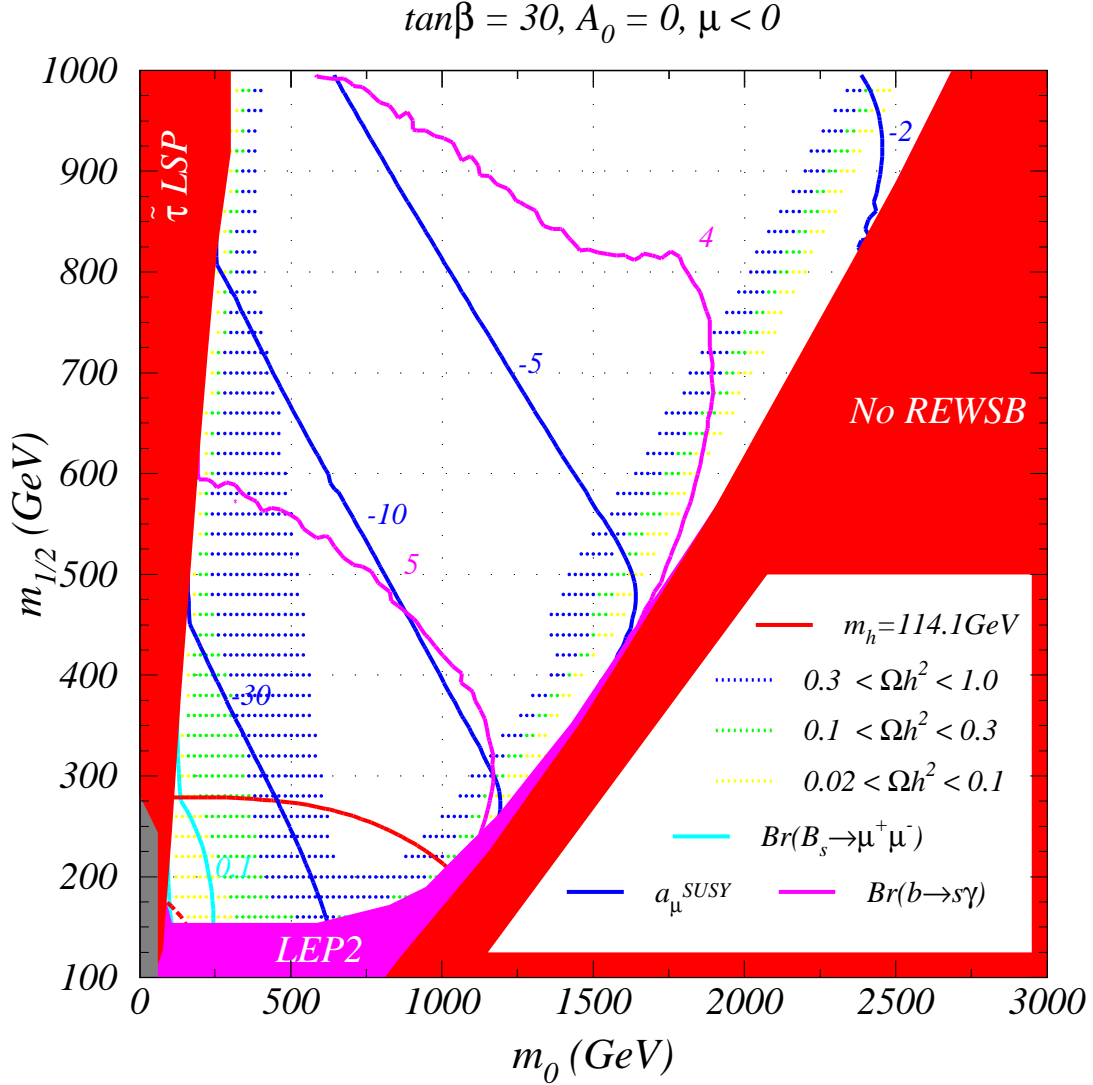


Figure 3: Same as Fig. 1, but for $\tan\beta = 30$ and $\mu < 0$. The light blue contour labeled 0.1 denotes where $B(B_s \rightarrow \mu^+ \mu^-) = 0.1 \times 10^{-7}$. In subsequent figures these branching fractions contours are all labeled in units of 10^{-7} .

from lower left with 60×10^{-10} , then proceed to 40, 20, 10, 5 and 2×10^{-10} . A fraction of the slepton annihilation region of relic density is excluded also by too large a value of δa_μ . Of course, a reasonable relic density may also be achieved in the stau co-annihilation and focus point regions of parameter space.

Next, we examine the mSUGRA parameter plane for very large values of $\tan\beta = 45$ and $\mu < 0$. If we take $\tan\beta$ much bigger than 45 for this sign of μ , the entire parameter space is excluded due to lack of REWSB. The gray and red regions are as in previous figures. The blue region is excluded because $m_A^2 < 0$, denoting again a lack of appropriate REWSB.

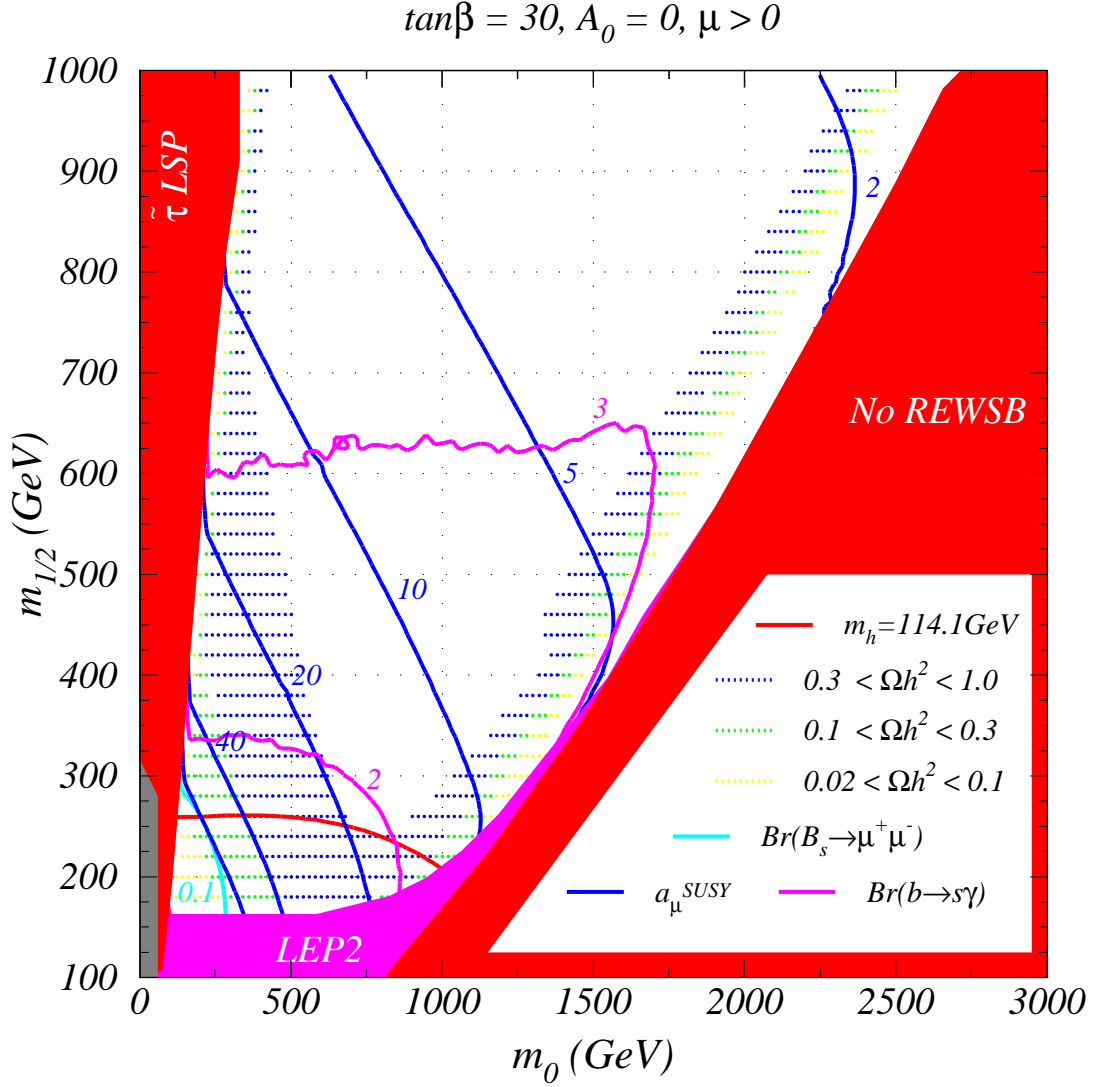


Figure 4: Same as Fig. 1, but for $\tan\beta = 30$ and $\mu > 0$.

The inner and outer red dashed lines are contours of $m_A = 100$ and $m_A = 200$ GeV, respectively. The former is roughly the lower bound on m_A from LEP experiments. In between these contours, h is not quite SM-like, and the mass bound from LEP may be somewhat lower than $m_h = 114.1$ GeV shown by the solid red contour, but outside the 200 GeV contour this bound should be valid.

The tiny black region in the figure is excluded by constraints[52] on the width of the Z boson (specifically, the decay $Z \rightarrow hA + HA$ leads to too large a value for Γ_Z). We also see that much of the lower-left region is excluded by too high a value of $BF(b \rightarrow s\gamma)$ and too low a value of δa_μ . In addition, in this plane, the experimental limit on $B_s \rightarrow \mu^+\mu^-$ enters the lower-left, where values exceeding 26×10^{-7} are obtained. It seems that in the

upper region which is favored by the $b \rightarrow s\gamma$ constraint, detection of $B_s \rightarrow \mu^+\mu^-$ at the Tevatron will be quite challenging.

In this figure, the relic density regions are qualitatively different from the lower $\tan\beta$ plots. A long diagonal strip running from lower-left to upper-right occurs because in this region, neutralinos annihilate very efficiently through s -channel A and H Higgs graphs, where the total Higgs widths are very large due to the large b and τ Yukawa couplings for the high value of $\tan\beta$ in this plot. Adjacent to this region are yellow and green shaded regions where neutralino annihilation is still dominated by the s -channel Higgs graphs, but in this case the annihilation is somewhat off-resonance. The A and H widths are so large, typically 20 – 60 GeV, that even if $|2m_{\tilde{Z}_1} - m_{A(H)}|$ is relatively large, efficient annihilation can still take place. The relic density changes so slowly on the flanks of the annihilation corridor that little fine tuning of parameters is needed to achieve a favored value of $\Omega_{\tilde{Z}_1} h^2$.

For the case of $\mu > 0$, $\tan\beta$ values ranging up to 60 can be allowed, although the mSUGRA parameter space becomes very limited for $\tan\beta \gtrsim 55$. Hence, we show in Fig. 6 the mSUGRA parameter space plane for $\tan\beta = 52$ and $\mu > 0$. In this parameter plane, the relic density annihilation corridor occurs near the boundary of the excluded $\tilde{\tau}_1$ LSP region. The width of the A and H Higgs scalars is very wide, ranging from 30 GeV for $m_{1/2} \sim 400$ GeV, to 110-130 GeV for $m_{1/2} \sim 2000$ GeV. Efficient s -channel annihilation through the Higgs poles can occur throughout much of the upper region of allowed parameter space. But the annihilation is not overly efficient due to the extreme breadth of the Higgs resonances. In fact, *none* of the entire parameter plane is excluded by $\Omega_{\tilde{Z}_1} h^2 > 1$! The change in $\Omega_{\tilde{Z}_1} h^2$ is so slow over almost the entire parameter plane that little fine-tuning occurs.

In much of the region with $m_{1/2} < 400$ GeV, the value of $BF(b \rightarrow s\gamma)$ is below 2×10^{-4} , so that some of the lower green relic density region where annihilation occurs through t -channel stau exchange is excluded. In contrast, the value of δa_μ is in the range of $10 - 40 \times 10^{-10}$, which is in accord with the E821 measurement. The value of m_h is almost always above 114.1 GeV, and the $BF(B_s \rightarrow \mu^+\mu^-)$ is always below 10^{-7} , and could (if at all) be detected with several years of main injector operation.

Aside from the somewhat low value of $BF(b \rightarrow s\gamma)$ in the lower left, much of this plane represents a very attractive area of mSUGRA model parameter space. If the model parameters are indeed in this range, the Tevatron signal for $B_s \rightarrow \mu^+\mu^-$ will be small, and $BF(b \rightarrow s\gamma)$ will turn out somewhat below the SM prediction, while δa_μ will be somewhat above the SM value.

4. Conclusions

In this paper, we have presented updated constraints on the mSUGRA model from *i.*) the LEP2 constraints on sparticle and Higgs boson masses, *ii.*) the neutralino relic density $\Omega_{\tilde{Z}_1} h^2$, *iii.*) the branching fraction $BF(b \rightarrow s\gamma)$, *iv.*) the muon anomalous magnetic moment a_μ and *v.*) the leptonic decay $B_s \rightarrow \mu^+\mu^-$. Putting all five constraints together, we find favored regions of parameter space which may be categorized by the mechanism for annihilating relic neutralinos in the early universe:

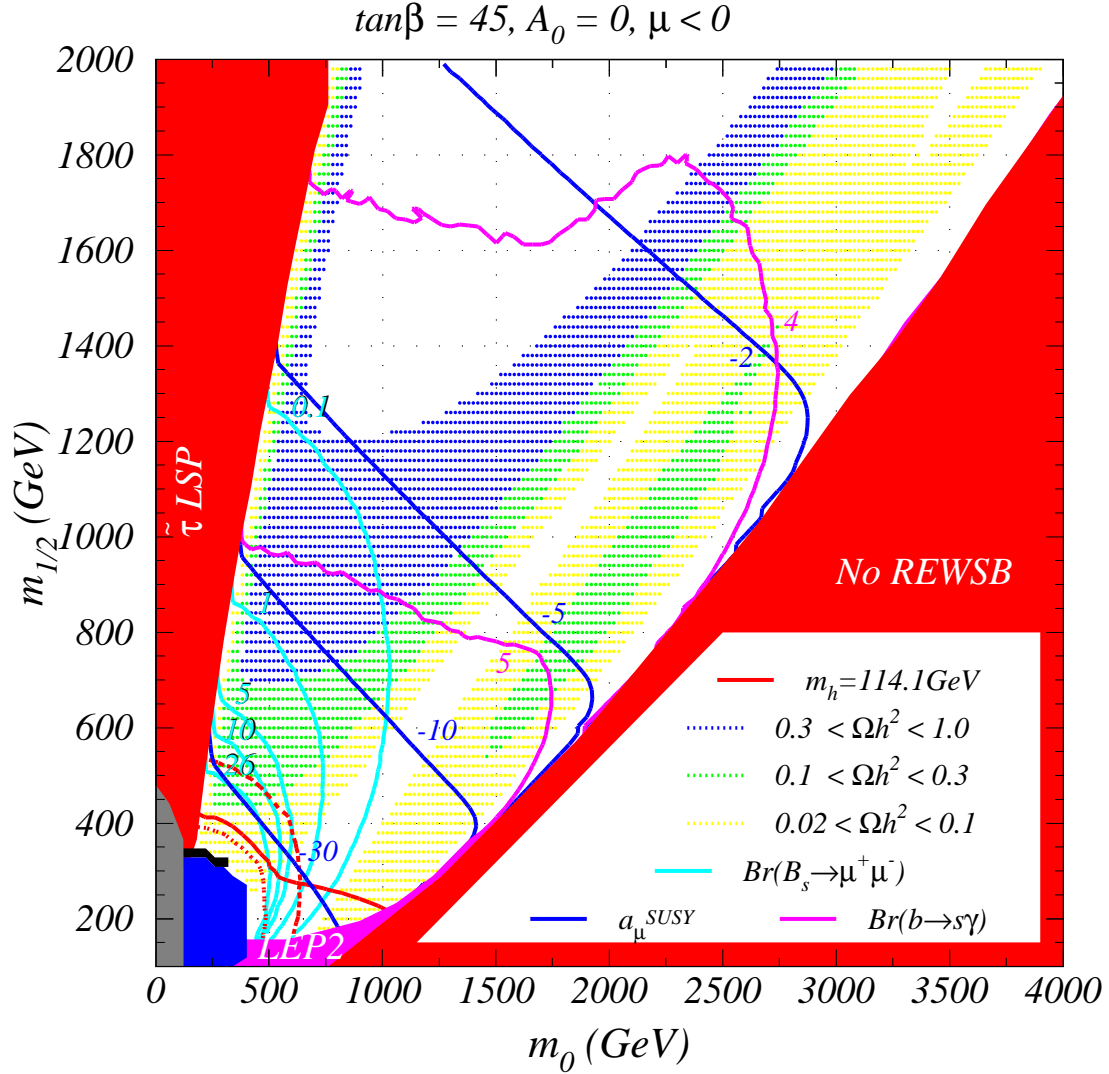


Figure 5: Same as Fig. 1, but for $\tan\beta = 45$ and $\mu < 0$. The inner and outer red dashed lines are contours of $m_A = 100$ and $m_A = 200$ GeV, respectively.

- **1.** annihilation through t -channel slepton exchange (low m_0 and $m_{1/2}$),
- **2.** the stau co-annihilation region (very low m_0 but large $m_{1/2}$),
- **3.** the focus point region (large m_0 but low to intermediate $m_{1/2}$) and
- **4.** the flanks of the neutralino s -channel annihilation via A and H corridor at large $\tan\beta$ when Γ_A and Γ_H are very large.

In previous years, there may have been a preference for region **1**. as offering the most natural channel for obtaining a reasonable value of relic density. However, recently much of

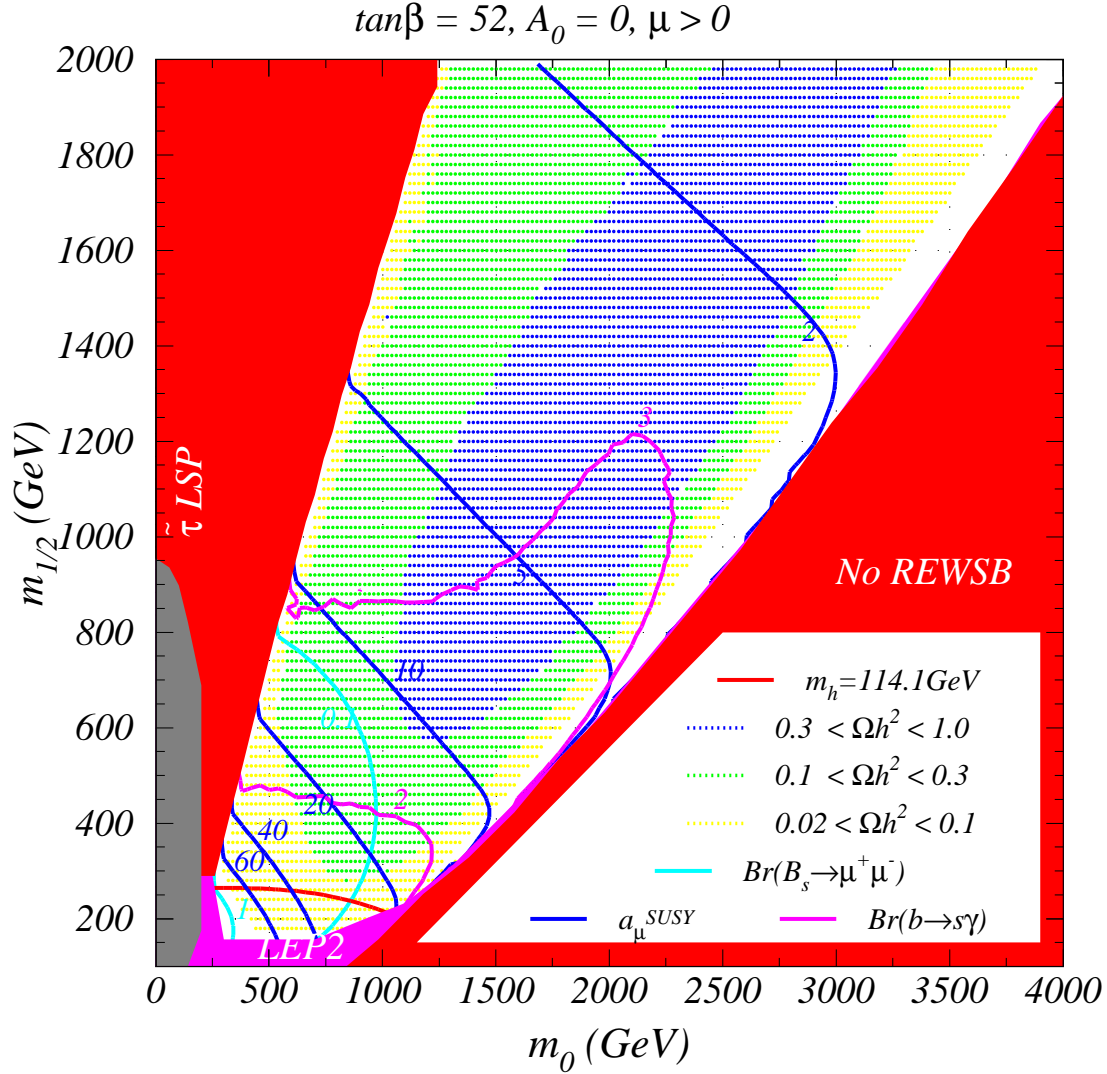


Figure 6: Same as Fig. 1, but for $\tan\beta = 52$ and $\mu > 0$.

this region is ruled out by a combination of LEP2 limits on m_h at low $\tan\beta$, too high (for $\mu < 0$) or too low (for $\mu > 0$ and large $\tan\beta$) a value of $BF(b \rightarrow s\gamma)$, and too low a value of a_μ (for $\mu < 0$ and intermediate to large $\tan\beta$). In addition, the CDF $BF(B_s \rightarrow \mu^+\mu^-)$ constraint is starting to become important for $\mu < 0$ and large $\tan\beta$. Nevertheless, some of region 1 remains viable, especially for $\mu > 0$, where we expect a lightest Higgs boson just beyond the bounds from LEP2.

The stau co-annihilation region[47] **2.** is intriguing because one can always take $m_{1/2}$ large enough for any $\tan\beta$ value to evade constraints on deviations from SM predictions. However, this region is exceptionally narrow in the parameter m_0 , and slight deviations cause either too high or too low a value of relic density. This indicates a high degree of

fine-tuning in the determination of the relic density in this region.

The focus point region[50] **3.** also leads to a reasonable relic density, this time because the higgsino component of \tilde{Z}_1 is large enough that efficient annihilation can occur to WW , ZZ and ZH states. It may also be preferable based on possibly low electroweak fine-tuning, and because matter scalar masses are high enough to offer some degree of suppression of SUSY induced FC and CP violating processes[50]. This region also suffers some degree of fine-tuning of the relic density, since too high or too low a higgsino component of \tilde{Z}_1 can result in too low or too high a value of relic density. For $\tan\beta \sim 10$ and $\mu > 0$, the focus point region is in accord with all constraints. For $\mu < 0$, the focus point region usually gives too high a value of $BF(b \rightarrow s\gamma)$; for $\mu > 0$, we would expect ultimately experiment to measure a somewhat lower value of $BF(b \rightarrow s\gamma)$ than the SM prediction, and a somewhat higher value of a_μ .

Finally, at very large $\tan\beta \sim 45 - 55$ there can exist wide regions of parameter space where $\tilde{Z}_1\tilde{Z}_1$ annihilation can occur in the early universe through very broad s -channel A and H resonances, giving rise to a reasonable value of relic density[20, 18]: region **4.** Unfortunately, much of this region is excluded for $\mu < 0$ by too large a value of $BF(b \rightarrow s\gamma)$. Here also a rather low a value of a_μ less than the SM prediction is generated. In this case, very large values of m_0 and $m_{1/2}$ are needed to escape experimental constraints, perhaps placing the SUSY spectrum in conflict with naturalness bounds[53].

For very large $\tan\beta$ and $\mu > 0$, however, broad regions of parameter space can be found with a reasonable relic density, and also which are in accord with all other low energy constraints. In this region, we expect $BF(b \rightarrow s\gamma)$ somewhat below the SM prediction, and a_μ somewhat above the SM prediction. The current $BF(b \rightarrow s\gamma)$ measurement suggest $m_{1/2}$ values $\gtrsim 500$ GeV, giving rise to sparticles typically at the TeV scale or beyond.

To summarize these various regions, we present in Table 1 five parameter space points indicating the SUSY spectrum that might occur in each region. We also list the relic density, $BF(b \rightarrow s\gamma)$, a_μ and $BF(B_s \rightarrow \mu^+\mu^-)$ values.

Point 1 occurs in region **1.**, and is characterized by light sparticle masses, especially tau sleptons. The light Higgs scalar h is slightly beyond the LEP2 bound. The search channel at the Fermilab Tevatron would be $p\bar{p} \rightarrow \tilde{W}_1\tilde{Z}_2X$, with $\tilde{Z}_2 \rightarrow \tau\tilde{\tau}_1$ and $\tilde{W}_1 \rightarrow \tilde{\tau}\nu_\tau$ though detection appears to be difficult[54]. The CERN LHC would be awash in signals[55], and many new SUSY states would be accessible to a linear collider (LC) with $\sqrt{s} \simeq 500 - 800$ GeV[56].

Point 2 is in the stau co-annihilation region **2.**, but at low enough $m_{1/2}$ that t -channel stau exchange is still important in the $\tilde{Z}_1\tilde{Z}_1$ annihilations. It is characterized by a rather small mass gap between $\tilde{\tau}_1$ and \tilde{Z}_1 . Only the Higgs boson h would be observable at the Tevatron. At the LHC, a variety of leptonic signatures would occur in gluino and squark cascade decays, including a high rate of τ production. The LC would have to operate slightly above $\sqrt{s} \sim 500$ GeV to access even the first SUSY states.

Point 3 in the focus point region **3.** has TeV scale scalars, but light \tilde{W}_1 and \tilde{Z}_2 . The LSP is a mixture of gaugino-higgsino. The \tilde{W}_1 decays into three bodies dominated by W^* exchange, and the \tilde{Z}_2 decay is dominated by Z^* exchange. Because this point is in the

region with small $|\mu|$ (but with a not too small $m_{\tilde{W}_1} - m_{\tilde{Z}_1}$), a low rate of trilepton events may be accessible to Fermilab Tevatron experiments. At the CERN LHC, $\tilde{g}\tilde{g}$ and $\tilde{W}_1\tilde{Z}_2$ production would be dominant. A LC would be able to find most of the charginos and neutralinos, since these are the lowest lying states.

Point 4a lies in region **4.** on the edge of the Higgs annihilation corridor for large $\tan\beta$ and $\mu < 0$. To evade constraints, the SUSY spectrum is very heavy: only the Higgs h would be seen at the Tevatron or a LC, and in fact it would even be challenging to discover SUSY at the LHC. This point is disfavored by naturalness arguments.

Point 4b also in region **4.** lies in the Higgs annihilation corridor for large $\tan\beta$ and $\mu > 0$. A significantly lighter spectrum can be tolerated than in the 4a case, although SUSY scalars are still in the TeV range. Only the h would be accessible at the Tevatron. SUSY signals corresponding to point 4b should be readily visible at the LHC, although a LC with $\sqrt{s} > 1$ TeV would be required to access even the lowest lying SUSY states.

To summarize, we find the five constraints considered in this paper to be highly restrictive. Together, they rule out large regions of parameter space of the mSUGRA model, including much of the region where t -channel slepton annihilation of neutralinos occurs in the early universe. The surviving regions **1.-4.** have distinct characteristics of their SUSY spectrum, and should lead to distinct SUSY signatures at colliders.

Acknowledgments

This research was supported in part by the U.S. Department of Energy under contracts number DE-FG02-97ER41022 and DE-FG03-94ER40833, and by Fundação de Amparo à Pesquisa do Estado de São Paulo (FAPESP).

References

- [1] For recent reviews, see *e.g.* S. Martin, in *Perspectives on Supersymmetry*, edited by G. Kane (World Scientific), [hep-ph/9709356](#); M. Drees, [hep-ph/9611409](#); J. Bagger, [hep-ph/9604232](#); X. Tata, *Proc. IX J. Swieca Summer School*, J. Barata, A. Malbousson and S. Novaes, Eds., [hep-ph/9706307](#); S. Dawson, *Proc. TASI 97*, J. Bagger, Ed., [hep-ph/9712464](#).
- [2] A. Chamseddine, R. Arnowitt and P. Nath, *Phys. Rev. Lett.* **49** (1982) 970; R. Barbieri, S. Ferrara and C. Savoy, *Phys. Lett.* **B 119** (1982) 343; L. J. Hall, J. Lykken and S. Weinberg, *Phys. Rev.* **D 27** (1983) 2359; for a review, see H. P. Nilles, *Phys. Rept.* **110** (1984) 1.
- [3] M. Dine and A. E. Nelson, *Phys. Rev.* **D 48** (1993) 1277; M. Dine, A. E. Nelson and Y. Shirman, *Phys. Rev.* **D 51** (1995) 1362; M. Dine, A. E. Nelson, Y. Nir and Y. Shirman, *Phys. Rev.* **D 53** (1996) 2658; for a review, see G. F. Giudice and R. Rattazzi, *Phys. Rept.* **322** (1999) 419.
- [4] L. Randall and R. Sundrum, *Nucl. Phys.* **B 557** (1999) 79; G. F. Giudice, M. A. Luty, H. Murayama and R. Rattazzi, *J. High Energy Phys.* **12** (1998) 027.
- [5] D. E. Kaplan, G. D. Kribs and M. Schmaltz, *Phys. Rev.* **D 62** (2000) 035010; Z. Chacko, M. A. Luty, A. E. Nelson and E. Ponton, *J. High Energy Phys.* **0001** (2000) 003.

- [6] S. K. Soni and H. A. Weldon, *Phys. Lett. B* **126** (1983) 215; V. Kaplunovsky and J. Louis, *Phys. Lett. B* **306** (1993) 269.
- [7] K. Choi, J. S. Lee and C. Munoz, *Phys. Rev. Lett.* **80** (1998) 3686.
- [8] H. Baer, F. Paige, S. Protopopescu and X. Tata, [hep-ph/0001086](#).
- [9] S. Heinemeyer, W. Hollik and G. Weiglein, [hep-ph/0002213](#).
- [10] D. Pierce, J. Bagger, K. Matchev and R. Zhang, *Nucl. Phys. B* **491** (1997) 3.
- [11] M. E. Gomez, G. Lazarides and C. Pallis, [hep-ph/0203131](#).
- [12] J. Ellis, K. Olive and Y. Santoso, [hep-ph/0202110](#).
- [13] L. Roszkowski, R. Ruiz de Austri and T. Nihei, *J. High Energy Phys.* **0108** (2001) 024.
- [14] A. Djouadi, M. Drees and J. L. Kneur, *J. High Energy Phys.* **0108** (2001) 055.
- [15] W. de Boer, M. Huber, C. Sander and D. I. Kazakov, *Phys. Lett. B* **515** (2001) 283.
- [16] S. Kraml, talk given at SUSY 2002, http://www.desy.de/~susy02/pa.1b/kraml_susy.ps.gz.
- [17] H. Baer, C. Balázs and A. Belyaev, *J. High Energy Phys.* **0203** (2002) 042.
- [18] H. Baer and M. Brhlik, *Phys. Rev. D* **53** (1996) 597 and *Phys. Rev. D* **57** (1998) 576; V. Barger and C. Kao, *Phys. Rev. D* **57** (1998) 3131 and *Phys. Lett. B* **518** (2001) 117; DarkSUSY, by P. Gondolo and J. Edsjö, [astro-ph/0012234](#); H. Baer, M. Brhlik, M. A. Diaz, J. Ferrandis, P. Mercadante, P. Quintana and X. Tata, *Phys. Rev. D* **63** (2001) 015007.
- [19] G. Belanger, F. Boudjema, A. Pukhov and A. Semenov, [hep-ph/0112278](#).
- [20] M. Drees and M. Nojiri, *Phys. Rev. D* **47** (1993) 376.
- [21] P. Nath and R. Arnowitt, *Phys. Rev. Lett.* **70** (1993) 3696; R. Arnowitt and P. Nath, *Phys. Lett. B* **437** (1998) 344.
- [22] J. R. Ellis, T. Falk, G. Ganis, K. A. Olive and M. Srednicki, *Phys. Lett. B* **510** (2001) 236.
- [23] A.B. Lahanas and V.C. Spanos, *Eur. Phys. J. C* **23** (2002) 185; see also, A.B. Lahanas, D.V. Nanopoulos and V.C. Spanos, *Phys. Rev. D* **62** (2000) 023515.
- [24] F. Abe *et al.*, (CDF Collaboration), *Phys. Rev. D* **57** (1998) 3811.
- [25] K. Babu and C. Kolda, *Phys. Rev. Lett.* **84** (2000) 228; A. Dedes, H. Dreiner and U. Nierste, *Phys. Rev. Lett.* **87** (2001) 251804; R. Arnowitt, B. Dutta, T. Kamon and M. Tanaka, [hep-ph/0203069](#).
- [26] Joint HEP2 Supersymmetry Working Group, *Combined Chargino Results, up to 208 GeV*, http://alephwww.cern.ch/lepsusy/www/inos_moriond01/charginos.pub.html.
- [27] Joint HEP2 Supersymmetry Working Group, *Combined LEP Selectron/Smuon/Stau Results, 183-208 GeV*, http://alephwww.cern.ch/~ganis/SUSYWG/SLEP/sleptons_2k01.html.
- [28] LEP Higgs Working Group Collaboration, [hep-ex/0107030](#).
- [29] See *e.g.* W. L. Freedman, *Phys. Rev.* **333** (2000) 13.
- [30] CompHEP v.33.23, by A. Pukhov *et al.*, [hep-ph/9908288](#).
- [31] P. Gondolo and G. Gelmini, *Nucl. Phys. B* **360** (1991) 145; J. Edsjö and P. Gondolo, *Phys. Rev. D* **56** (1997) 1879.

- [32] K. Abe *et al.* (Belle Collaboration), *Phys. Lett. B* **511** (2001) 151.
- [33] D. Cronin-Hennessy *et al.* (Cleo Collaboration), *Phys. Rev. Lett.* **87** (2001) 251808.
- [34] R. Barate *et al.* (Aleph Collaboration), *Phys. Lett. B* **429** (1998) 169.
- [35] P. Gambino and M. Misiak, *Nucl. Phys. B* **611** (2001) 338.
- [36] H. Baer and M. Brhlik, *Phys. Rev. D* **55** (1997) 3201; H. Baer, M. Brhlik, D. Castaño and X. Tata, *Phys. Rev. D* **58** (1998) 015007.
- [37] H. Anlauf, *Nucl. Phys. B* **430** (1994) 245.
- [38] G. Degrossi, P. Gambino and G. Giudice, *J. High Energy Phys.* **0012** (2000) 009.
- [39] M. Carena, D. Garcia, U. Nierste and C. Wagner, *Phys. Lett. B* **499** (2001) 141.
- [40] H. N. Brown *et al.*, (E821 Collaboration), *Phys. Rev. Lett.* **86** (2001) 2227.
- [41] A. Czarnecki and W. Marciano, *Phys. Rev. D* **64** (2001) 013014. This uses the analysis of M. Davier and A. Höcker, *Phys. Lett. B* **435** (1998) 427 which in turn uses τ decay data to reduce the error on the hadronic vacuum polarization. See also S. Narison, *Phys. Lett. B* **513** (2001) 53.
- [42] M. Knecht and A. Nyffeler, *Phys. Rev. D* **65** (2002) 073034; M. Knecht, A. Nyffeler, M. Perrottet and E. De Rafael, *Phys. Rev. Lett.* **88** (2002) 071802; M. Hayakawa and T. Kinoshita, [hep-ph/0112102](#); I. Blokland, A. Czarnecki and K. Melnikov, *Phys. Rev. Lett.* **88** (2002) 071803.
- [43] K. Melnikov, *Int. J. Mod. Phys. A* **16** (2001) 4591. His updated analysis of the SM value of δa_μ was presented at the High Energy Physics Seminar, University of Hawaii, March 2002.
- [44] F. Jegerlehner, [hep-ph/0104304](#).
- [45] H. Baer, C. Balázs, J. Ferrandis and X. Tata, *Phys. Rev. D* **64** (2001) 035004.
- [46] J. K. Mizukoshi, X. Tata and Y. Wang (in preparation).
- [47] J. Ellis, T. Falk and K. Olive, *Phys. Lett. B* **444** (1998) 367; J. Ellis, T. Falk, K. Olive and M. Srednicki, *Astropart. Phys.* **13** (2000) 181.
- [48] J. Ellis and K. Olive, *Phys. Lett. B* **514** (2002) 114.
- [49] J. Feng, K. Matchev and F. Wilczek, *Phys. Lett. B* **482** (2000) 388 and *Phys. Rev. D* **63** (2001) 045024.
- [50] J. Feng, K. Matchev and T. Moroi, *Phys. Rev. D* **61** (2000) 075005.
- [51] M. Carena *et al.*, [hep-ph/0010338](#).
- [52] H. Baer, M. Drees and X. Tata, *Phys. Rev. D* **41** (1990) 3414; J. Ellis, G. Ridolfi and F. Zwirner, *Phys. Lett. B* **237** (1990) 423.
- [53] G. W. Anderson and D. J. Castaño, *Phys. Lett. B* **347** (1995) 300 and *Phys. Rev. D* **52** (1995) 1693.
- [54] H. Baer, C. H. Chen, M. Drees, F. Paige and X. Tata, *Phys. Rev. D* **58** (1998) 075008; V. Barger, C. Kao and T. Li, *Phys. Lett. B* **433** (1998) 328; V. Barger and C. Kao, *Phys. Rev. D* **60** (1999) 115015; K. Matchev and D. Pierce, *Phys. Rev. D* **60** (1999) 075004 and *Phys. Lett. B* **467** (1999) 225; J. Lykken and K. Matchev, *Phys. Rev. D* **61** (2000) 015001; H. Baer, M. Drees, F. Paige, P. Quintana and X. Tata, *Phys. Rev. D* **61** (2000) 095007; for a review, see S. Abel *et al.* (SUGRA Working Group Collaboration), [hep-ph/0003154](#).

- [55] H. Baer, C. H. Chen, F. Paige and X. Tata, *Phys. Rev. D* **52** (1995) 2746 and *Phys. Rev. D* **53** (1996) 6241; H. Baer, C. H. Chen, M. Drees, F. Paige and X. Tata, *Phys. Rev. D* **59** (1998) 055014; S. Abdullin *et al.* (CMS Collaboration), [hep-ph/9806366](#).
- [56] H. Baer, R. Munroe and X. Tata, *Phys. Rev. D* **54** (1996) 6735; for a review, see T. Abe *et al.* (American Linear Collider Working Group Collaboration), [hep-ex/0106056](#); J. A. Aguilar-Saavedra *et al.* (ECFA/DESY LC Physics Working Group Collaboration), [hep-ph/0106315](#).

Table 1: Representative weak scale sparticle masses (in GeV units) and parameters for five selected mSUGRA models. We use $A_0 = 0$ and $m_t = 175$ GeV. The value of μ is also shown since it is sometimes regarded as a measure of fine tuning.

parameter	value				
<i>point</i>	1	2	3	4a	4b
m_0	100	165	1200	2750	800
$m_{1/2}$	300	550	250	1800	800
$\tan(\beta)$	10	10	10	45	52
$sgn(\mu)$	1	1	1	-1	1
$m_{\tilde{g}}$	701.4	1225.6	658.0	3810.8	1757.6
$m_{\tilde{u}_L}$	630.7	1099.1	1271.1	4185.0	1715.3
$m_{\tilde{u}_R}$	611.1	1060.0	1269.1	4080.7	1662.4
$m_{\tilde{d}_L}$	635.6	1102.0	1273.6	4185.8	1717.1
$m_{\tilde{d}_R}$	610.0	1055.7	1269.6	4067.4	1656.5
$m_{\tilde{b}_1}$	584.9	1020.8	1072.4	3501.7	1484.4
$m_{\tilde{b}_2}$	610.7	1053.4	1260.8	3537.6	1539.4
$m_{\tilde{t}_1}$	471.7	858.5	825.2	3213.2	1328.2
$m_{\tilde{t}_2}$	648.1	1064.0	1084.3	3529.6	1533.6
$m_{\tilde{\nu}_e}$	216.4	396.7	1203.1	2972.3	952.4
$m_{\tilde{e}_L}$	230.4	404.5	1205.7	2973.4	955.8
$m_{\tilde{e}_R}$	155.5	264.8	1201.7	2822.1	851.7
$m_{\tilde{\nu}_\tau}$	215.6	395.4	1198.0	2750.8	834.0
$m_{\tilde{\tau}_1}$	147.5	257.6	1191.0	2320.8	524.2
$m_{\tilde{\tau}_2}$	233.4	405.2	1200.8	2752.6	847.9
$m_{\tilde{Z}_1}$	117.5	225.1	88.6	785.0	336.2
$m_{\tilde{Z}_2}$	215.1	416.9	144.1	1235.1	620.2
$m_{\tilde{Z}_3}$	398.5	668.1	198.2	1249.2	848.7
$m_{\tilde{Z}_4}$	417.8	682.8	260.9	1461.7	862.3
$m_{\tilde{W}_1}$	214.7	416.9	136.5	1234.5	620.3
$m_{\tilde{W}_2}$	418.0	682.6	260.3	1461.7	862.5
m_h	114.7	119.0	114.4	123.9	121.5
m_H	443.9	766.5	1204.9	1495.2	810.1
m_A	443.3	765.7	1203.9	1494.2	809.5
m_{H^+}	450.7	770.4	1207.4	1498.4	816.5
μ	392.0	664.9	188.7	-1247.2	845.8
Ωh^2	0.232	0.218	0.262	0.210	0.181
$BF(b \rightarrow s\gamma) \times 10^4$	3.12	3.46	3.20	3.92	2.85
$a_\mu^{SUSY} \times 10^{10}$	22.6	7.13	2.65	-1.48	10.2
$BF(B_s \rightarrow \mu^+ \mu^-) \times 10^7$	0.0399	0.0389	0.0384	0.0306	0.0870